

Article

Continuous-Wave Crystalline Laser at 714 nm via Stimulated Raman Scattering and Sum Frequency Generation

Chien-Yen Huang¹, Bo-Cheng Guo¹, Zi-Xuan Zheng¹, Chia-Han Tsou¹, Hsing-Chih Liang² 
and Yung-Fu Chen^{1,*} 

¹ Department of Electrophysics, National Yang Ming Chiao Tung University, Hsinchu 30010, Taiwan; so3355589.sc09@nycu.edu.tw (C.-Y.H.); kuobobo8694.sc10@nycu.edu.tw (B.-C.G.); qazwsxlas02.sc09@nycu.edu.tw (Z.-X.Z.); chtsou@nycu.edu.tw (C.-H.T.)

² Institute of Optoelectronic Science, National Taiwan Ocean University, Keelung 20224, Taiwan; hcliang@email.ntou.edu.tw

* Correspondence: yfchen@nycu.edu.tw

Abstract: A compact high-power continuous-wave (CW) laser at 714 nm is originally developed via intracavity stimulated Raman scattering (SRS) and sum frequency generation (SFG). The fundamental wave at 1342 nm and the first-Stokes Raman wave at 1525 nm are generated by using a Nd:YVO₄ and a undoped YVO₄ crystals, respectively. Compared to the self-Raman laser, the separation of the gain media for generating the fundamental and Raman waves can effectively reduce the thermal lens effect in the Nd:YVO₄ crystal and efficiently enhance the SRS in the undoped YVO₄ crystal. Furthermore, the undoped YVO₄ crystal is coated to act as a high-reflection mirror for minimizing the cavity losses. At a pump power of 40 W, the output power at 714 nm can reach 1.8 W. The present compact design for CW laser source at 714 nm is believed to be practically useful for laser cooling and trapping of radium.



Citation: Huang, C.-Y.; Guo, B.-C.; Zheng, Z.-X.; Tsou, C.-H.; Liang, H.-C.; Chen, Y.-F. Continuous-Wave Crystalline Laser at 714 nm via Stimulated Raman Scattering and Sum Frequency Generation. *Crystals* **2022**, *12*, 1046. <https://doi.org/10.3390/cryst12081046>

Academic Editor: Sergei N. Smetanin

Received: 26 June 2022

Accepted: 26 July 2022

Published: 28 July 2022

Publisher's Note: MDPI stays neutral with regard to jurisdictional claims in published maps and institutional affiliations.



Copyright: © 2022 by the authors. Licensee MDPI, Basel, Switzerland. This article is an open access article distributed under the terms and conditions of the Creative Commons Attribution (CC BY) license (<https://creativecommons.org/licenses/by/4.0/>).

Keywords: stimulated Raman scattering; continuous-wave laser; Nd:YVO₄ crystal

1. Introduction

Solid-state crystalline lasers with intracavity stimulated Raman scattering (SRS) have been identified as a practical way for widely extending output wavelengths [1–8]. Diode-pumped Nd-doped crystalline Raman lasers have been efficiently realized in the near infrared spectral region of 1.1–1.2 μm to develop high-power visible light sources via sum frequency generation (SFG) or second harmonic generation (SHG) in a nonlinear crystal [9–16]. In addition to the spectrum of 1.1–1.2 μm , Nd-doped solid-state Raman lasers in the eye-safe spectral region of 1.5 μm can be achieved by the first-Stokes Raman shift generated from 1.3- μm fundamental emission. Up to now, SRS gain media in Nd-doped solid-state eye-safe lasers mainly consisted of YVO₄ [17], GdVO₄ [18], SrWO₄ [19], BaWO₄ [20], and KGW [21], and so on. Nd-doped vanadate crystals such as GdVO₄, YVO₄, and LuVO₄ are especially classified as the self-Raman crystals on the grounds that they can generate the fundamental and Raman Stokes waves simultaneously. Since the gain coefficient of Nd-doped crystals at 1.3 μm was much smaller than that at 1.1 μm , almost eye-safe Raman lasers were realized in the Q-switched operation. The continuous-wave (CW) eye-safe Raman operation was first accomplished recently by using the in-band pumping and composite Nd: YVO₄ crystal [22].

A high-power CW light source at 714 nm is important for exploring the spectroscopic characteristics of atomic and ionic radium isotopes [23,24]. The 714 nm laser is used to drive the ¹S₀-³P₁ inter-combination transition in radium with the power level about 1.0 W, depending on experimental setup. Nowadays, the CW laser source at 714 nm is usually based on a Ti:sapphire ring laser. In this work, we originally accomplish a CW high-power 714 nm laser via SFG of the 1342 nm fundamental wave and the 1525 nm

stimulated Raman wave. To reduce the thermal lensing effect, the laser and Raman gain media are separated by individually exploiting a Nd-doped and a undoped YVO₄ crystals, respectively. Furthermore, a separate cavity is designed to enhance the SRS for lowering the lasing threshold of the Raman wave at 1525 nm. To minimize the cavity losses, the highly reflective mirror of the SRS cavity is achieved by depositing a dichroic coating on the end facet of the undoped YVO₄ crystal. The second facet is coated to be highly reflective at 714 nm to avoid the backward generation penetrating into the Raman and laser crystals. Note that the first idea for depositing a mirror coating on a laser crystal could date back to the work by Maiman [25]. We explored two types of arrangements for the Nd:YVO₄ and YVO₄ crystals with both *c*-axes to be parallel and perpendicular to each other. By using the traditional 808 nm pumped diode at a pump power of 40 W, the output power at the 714 nm SFG can be up to 1.8 W.

2. Cavity Design and Experimental Setup

The crystallographic structure of Nd:YVO₄ crystal is categorized into the D_{4h} tetragonal space group of the zircon type. The strongest Raman line corresponding to the internal vibrations of VO₄³⁻ group is near 890 cm⁻¹. The Raman line of 890 cm⁻¹ can shift the fundamental wave of 1342 nm to the first-Stokes wave of 1525 nm. Here, we developed a compact cavity to generate the fundamental field at 1342 nm and the first-Stokes Raman field at 1525 nm. Within the cavity, an LBO crystal was used to perform the SFG for attaining the coherent emission at 714 nm. Figure 1 shows the experimental setup for a diode-pumped Nd:YVO₄/YVO₄ Raman laser with a coupled cavity for simultaneous intracavity SRS and SFG to achieve a high-power 714 nm laser at the CW operation. The resonator for the fundamental wave was a concave-plano configuration. The concave input mirror with the radius of curvature of 100 mm was coated to be antireflective at 808 nm (reflectance < 0.2%) on the entrance facet and high-reflective at 1342 nm (reflectance > 99.9%) and a high-transmissive at 808 nm (transmittance > 95%) on the second facet. The laser gain medium was a 0.2 at.% Nd³⁺ doped *a*-cut Nd:YVO₄ crystal with dimensions of 3 × 3 × 15 mm³. Both end facets of the laser crystal were coated to be anti-reflective at 808 nm and 1342 nm. The laser crystal was wrapped in indium foil and mounted in a conduction-cooled copper block, and its temperature was maintained at 20 °C.

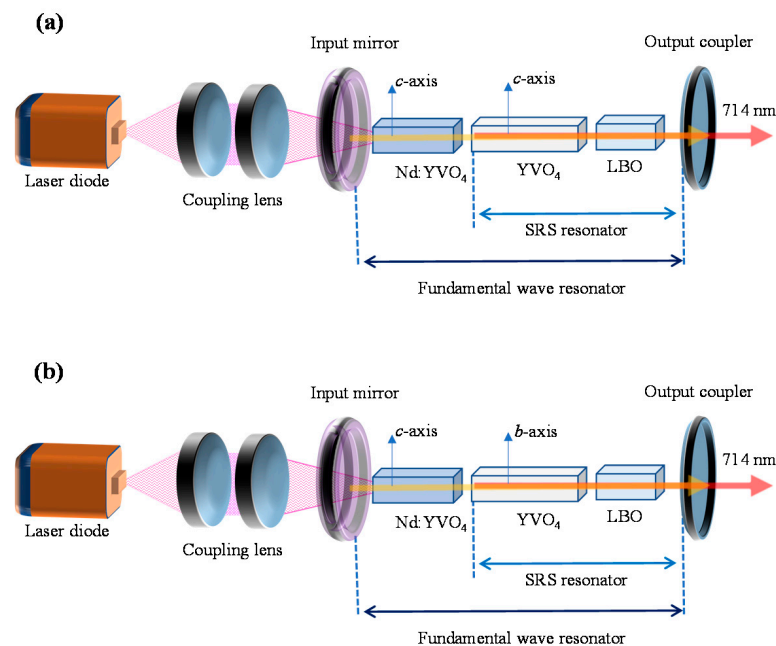


Figure 1. Experimental setup for a diode-pumped Nd:YVO₄/YVO₄ Raman laser to achieve a high-power 714 nm laser at the CW operation. Both *c*-axes (a) parallel (b) perpendicular to each other.

The gain medium for SRS was an undoped *a*-cut YVO₄ crystal with dimensions of 3 × 3 × 20 mm³. The first side (S1) of the undoped YVO₄ crystal was coated to be dichroic with high transmission at 1342 nm (transmittance > 99.0%) and high reflection at 1525 nm (reflectance > 99.5%). The second side (S2) of the undoped YVO₄ crystal had another dichroic coating to avoid the backward generation penetrating into the Raman and laser crystals. The transmittances of S2 at 1342 and 1525 nm were as high as 98%. The Raman crystals was also wrapped with an indium foil and then mounted in a conduction-cooled copper holder at a temperature of 20 °C. We explored two types of arrangements for the Nd:YVO₄ and YVO₄ crystals that are shown in Figure 1a,b for both *c*-axes to be parallel and perpendicular to each other, respectively. According to Porto notations, the spontaneous Raman scattering spectra of YVO₄ crystal relevant to the arrangements shown in Figure 1a,b are with $x(zz)\bar{x}$ and $x(yy)\bar{x}$ configurations that were measured by using NXR FT-Raman spectrum analyzer, shown in Figure 2. As can be seen, the spectra comprise of several sharp Raman lines corresponding to the internal vibrations of VO₄^{3−} group and external vibrations of VO₄^{3−} tetrahedra and Y³⁺ ions in YVO₄ unit cell. The spectra reveal that both Raman configurations in the YVO₄ crystal have different active vibration modes. The external vibration at 157 cm^{−1} (B_{1g}(1)), attributed to the O–Y–O bending mode, can be observed in both Raman configurations. On the other hand, the internal vibrations, which can be ascribed to the O–V–O bending and VO₄ stretching modes, located at higher frequencies—259 (B_{2g}), 376 (A_{1g}(1)), 487 (B_{1g}(3)), 816 (B_{1g}(4)), 838 (E_g(5)) and 890 cm^{−1} (A_{1g}(2))—can be completely observed in the $x(yy)\bar{x}$ configuration [26]. However, the modes at 487 and 816 cm^{−1} are not excited in the $x(zz)\bar{x}$ configuration. Nevertheless, both Raman spectra are dominated by the vibration mode at 890 cm^{−1}.

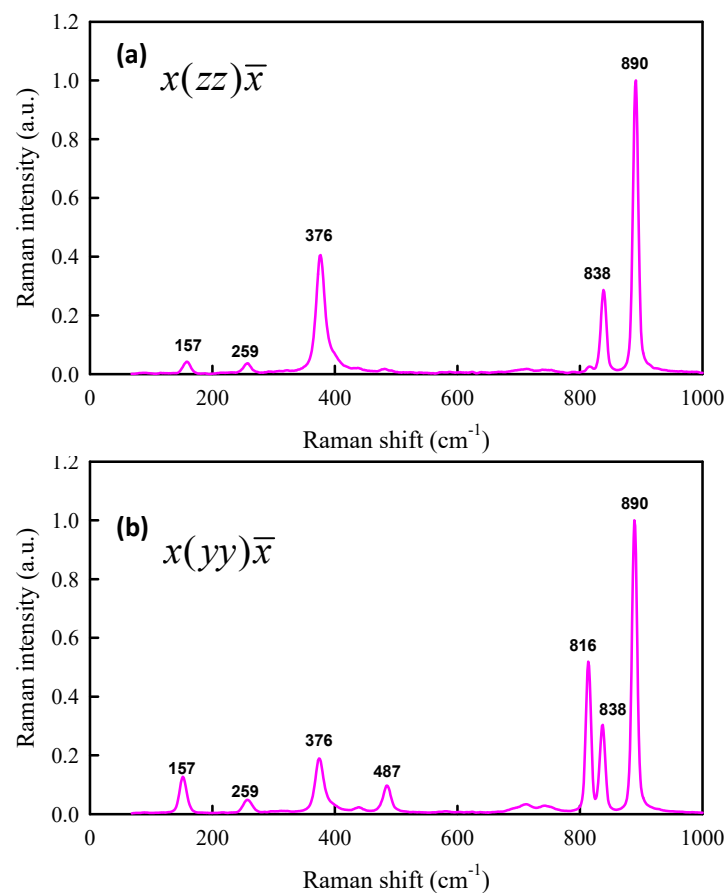


Figure 2. Spontaneous Raman scattering spectra with (a) $x(zz)\bar{x}$ and (b) $x(yy)\bar{x}$ configurations in *a*-cut YVO₄ crystal.

The intracavity SFG of 1342 and 1525 nm was performed by using a lithium triborate (LBO) crystal with a length of 8 mm and the cut angle at $\theta = 90^\circ$ and $\phi = 3.3^\circ$. The LBO crystal was also wrapped in indium foil and placed in a TEC-cooled copper block which ensured that the LBO crystal was maintained at the temperature for the best phase matching. Both sides of the LBO crystal were coated to be highly transmissive at 714, 1342 and 1525 nm (transmittance > 97%). The output coupler was a flat mirror. The first facet of the output coupler for the resonance was coated to be highly reflective within 1340–1530 nm (reflectance > 99.9%) and highly transmissive at 714 nm (transmittance > 95%). The other facet had an antireflection coating at 714 nm (reflectance < 0.2%). The laser crystal was pumped by a 40-W fiber coupled laser diode array with a central wavelength of 808 nm. The numerical aperture and core diameter for the coupled fiber of the pump source were 0.22 and 200 μm , respectively. The pump light from the fiber was re-imaged using a pair of achromatic lenses and focused into the Nd:YVO₄ crystal with a spot diameter of 500 μm .

3. Experimental Results and Discussion

Figure 3 shows the experimental result for the total output power versus the pump power at 808 nm with the cavity shown in Figure 1a for both *c*-axes to be parallel to each other. The 714 nm SFG and the fundamental and Raman output powers were individually recorded. The threshold pump powers for the fundamental and Raman waves were found to be approximately 1.5 W and 4.0 W, respectively. The output power at 714 nm was 1.25 W at a pump power of 40 W. Figure 4 shows the experimental result for the total output power versus the pump power at 808 nm with the cavity shown in Figure 1b for both *c*-axes to be perpendicular to each other. The threshold pump powers for the fundamental and Raman waves can be seen to be quite similar for both configurations with *c*-axes to be parallel and perpendicular to each other. Nevertheless, the conversion efficiency with the perpendicular configuration is obviously higher than that with the parallel one. The output power at 714 nm could reach 1.8 W at a pump power of 40 W.

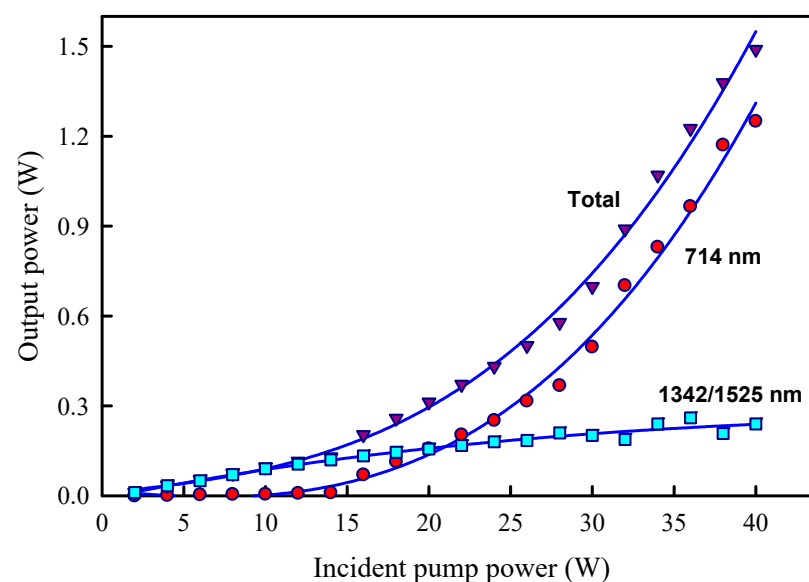


Figure 3. Experimental result for total output power, SFG output power, and fundamental and Raman output powers versus incident pump power with the cavity shown in Figure 1a.

The superior performance with the perpendicular configuration was speculated to arise from the thermal lensing effect in the YVO₄ crystal. The Raman cavity shown in Figure 1 can be seen to a flat-flat resonator which generally needs the thermal lens to bring it into geometric stability. For parallel and perpendicular configurations, the effective focal

lengths of the thermal lenses in the Raman crystal are denoted as f_{th}^{\parallel} and f_{th}^{\perp} , respectively. For an end-pumped cavity, f_{th}^{\parallel} and f_{th}^{\perp} can be expressed as [27–29]

$$\frac{1}{f_{th}^{\parallel}} = \frac{P_h}{2\pi K_c \omega_p^2} \left[\frac{dn_c}{dT} + (n_c - 1)\alpha_T \right] \quad (1)$$

$$\frac{1}{f_{th}^{\perp}} = \frac{P_h}{2\pi K_c \omega_p^2} \left[\frac{dn_b}{dT} + (n_b - 1)\alpha_T \right] \quad (2)$$

where P_h is the power of thermal load, K_c is the thermal conductivity, α_T is the thermal expansion coefficient, ω_p is the pump radius, and n_c and n_b are the refractive indices of the YVO_4 crystal with polarization along c and b axes, respectively. The terms of dn_c/dT and dn_b/dT are the thermal-optic coefficients of n_c and n_b , respectively. From Equations (1) and (2), the difference between f_{th}^{\parallel} and f_{th}^{\perp} mainly comes from the difference between dn_c/dT and dn_b/dT . For a undoped a -cut YVO_4 crystal, $dn_c/dT = 2.9 \times 10^{-6}/K$ and $dn_b/dT = 8.5 \times 10^{-6}/K$. Considering the contribution from $\alpha_T = 4.43 \times 10^{-6}/K$, the value of f_{th}^{\perp} can be found to be nearly two times smaller than that of f_{th}^{\parallel} . The effective area of the cavity mode induced by the thermal lens is approximately proportional to the square root of thermal focal length. Consequently, the mode area of the Raman wave in the perpendicular configuration was approximately $\sqrt{2}$ times smaller than that in the parallel configuration. The smaller the mode area, the higher the SRS efficiency. It is worth mentioning that the performance for both parallel and perpendicular configurations was explored for the first time.

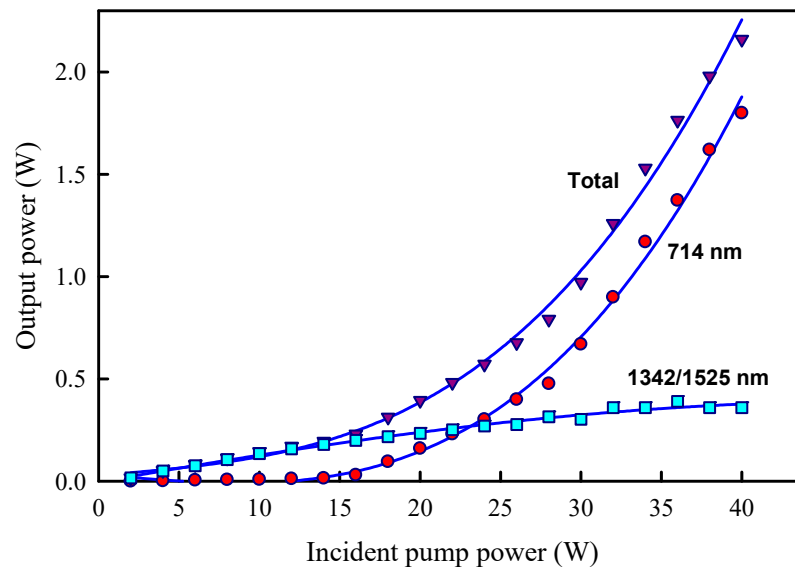


Figure 4. Experimental result for total output power, SFG output power, and fundamental and Raman output powers versus incident pump power with the cavity shown in Figure 1b.

We employed an optical spectrum analyzer with a resolution of 0.1 nm (Advantest Q8381A) to measure the lasing spectrum. Figure 5a shows the experimental result for the optical spectrum of the SFG wave at a pump power of 40 W with the parallel configuration. On the other hand, the optical spectrum of the fundamental and Raman waves at a pump power of 40 W is shown in Figure 5b. The beam quality M^2 factor for the output laser at 714 nm was found to be better than 3.5 at a pump power of 40 W. Note that the overall optical spectra and the beam quality were nearly the same for both parallel and perpendicular configurations. A good beam quality for the SFG wave could be obtained partly due to the end-pumping scheme and mainly due to Raman-induced beam cleanup. Based on

the present result, a higher output power at 714 nm could be achieved by enhancing the reflectivity for the fundamental and Raman fields on the cavity mirror and output coupler.

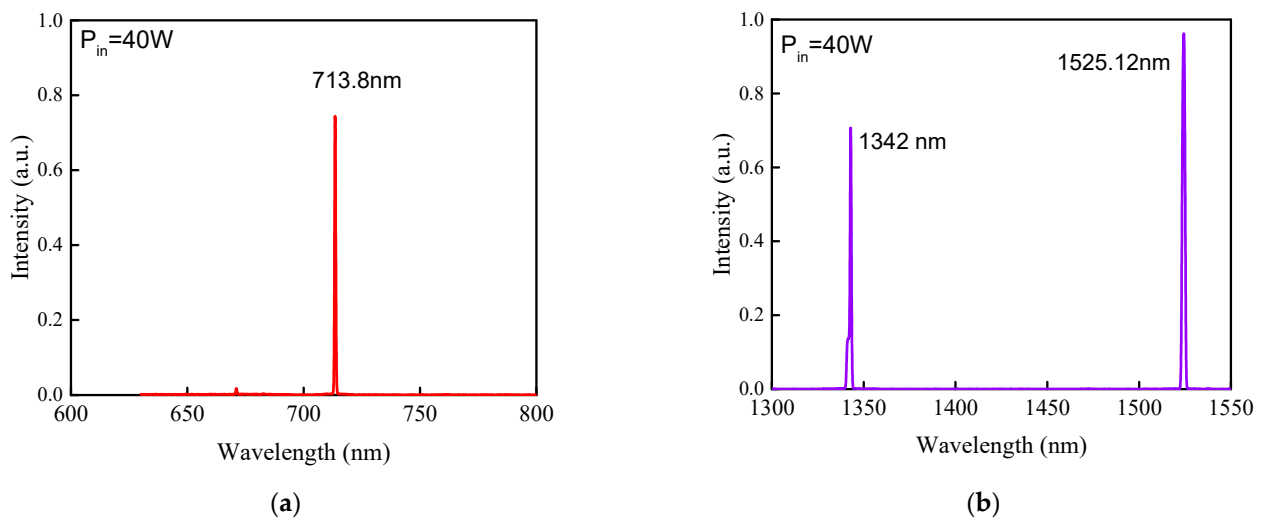


Figure 5. Experimental result for the optical spectrum of the output beam (a) SFG wave; (b) fundamental and Raman waves.

4. Conclusions

We have developed a high-power CW laser at 714 nm via intracavity SRS and SFG. Individual Nd:YVO₄ and undoped YVO₄ crystals were exploited to generate the fundamental wave at 1342 nm and the first-Stokes Raman wave at 1525 nm, respectively. Compared to the self-Raman resonator, the separate configuration of the present cavity could reduce the thermal lens effect in the Nd:YVO₄ crystal. Furthermore, we designed a compactly coupled cavity to accomplish the SRS process in the undoped YVO₄ crystal. To minimize the cavity losses of the SRS cavity, the Raman crystal was coated to act as a high-reflection mirror. At a pump power of 40 W, the output power at 714 nm obtained from the SFG of the fundamental and Raman waves could reach 1.8 W with the cavity both *c*-axes to be perpendicular to each other.

Author Contributions: Conceptualization, C.-Y.H. and Y.-F.C.; validation, Z.-X.Z. and B.-C.G.; formal analysis, C.-H.T. and H.-C.L.; resources, C.-Y.H. and Z.-X.Z.; writing—original draft preparation, Y.-F.C.; writing—review and editing, C.-Y.H., Z.-X.Z. and Y.-F.C.; supervision, Y.-F.C. All authors have read and agreed to the published version of the manuscript.

Funding: This work is supported by National Science and Technology Council, Taiwan (contract number 109-2112-M-009-015-MY3). This work is also supported by the Higher Education Sprout Project of the National Yang Ming Chiao Tung University and Ministry of Education (MOE), Taiwan.

Institutional Review Board Statement: Not applicable.

Informed Consent Statement: Not applicable.

Data Availability Statement: All of the data reported in the paper are presented in the main text. Any other data will be provided on request.

Conflicts of Interest: The authors declare no conflict of interest.

References

1. Ammann, E.O.; Falk, J. Stimulated Raman scattering at kHz pulse repetition rates. *Appl. Phys. Lett.* **1975**, *27*, 662–664. [[CrossRef](#)]
2. Basiev, T.T.; Powell, R.C. Solid-state Raman lasers. In *Handbook of Laser Technology and Applications*; Webb, C.E., Ed.; Ch. B1.7; The Institute of Physics: London, UK; Bristol, UK, 2003.
3. Cerný, P.; Jelinkova, H.; Zverev, P.G.; Basiev, T.T. Solid state lasers with Raman frequency conversion. *Prog. Quantum Electron.* **2004**, *28*, 113–143. [[CrossRef](#)]
4. Piper, J.A.; Pask, H.M. Crystalline Raman lasers. *IEEE J. Sel. Top. Quantum Electron.* **2007**, *13*, 692–704. [[CrossRef](#)]

5. Chen, Y.F. Efficient subnanosecond diode-pumped passively Q-switched Nd:YVO₄ self-stimulated Raman laser. *Opt. Lett.* **2004**, *29*, 1251–1253. [[CrossRef](#)] [[PubMed](#)]
6. Chen, Y.F. High-power diode-pumped actively Q-switched Nd:YVO₄ self-Raman laser: Influence of dopant concentration. *Opt. Lett.* **2004**, *29*, 1915–1917. [[CrossRef](#)]
7. Li, X.; Pask, H.M.; Lee, A.J.; Huo, Y.; Piper, J.A.; Spence, D.J. Miniature wavelength-selectable Raman laser: New insights for optimizing performance. *Opt. Express* **2011**, *19*, 25623–25631. [[CrossRef](#)]
8. Zhang, L.; Duan, Y.; Sun, Y.; Chen, Y.; Li, Z.; Zhu, H.; Zhang, G.; Tang, D. Passively Q-switched multiple visible wavelengths switchable YVO₄ Raman laser. *J. Lumin.* **2020**, *228*, 117650. [[CrossRef](#)]
9. Dekker, P.; Pask, H.M.; Spence, D.J.; Piper, J.A. Continuous-wave, intracavity doubled, self-Raman laser operation in Nd:GdVO₄ at 586.5 nm. *Opt. Express* **2007**, *15*, 7038–7046. [[CrossRef](#)]
10. Zhu, H.; Duan, Y.; Zhang, G.; Huang, C.; Wei, Y.; Chen, W.; Huang, Y.; Ye, N. Yellow-light generation of 5.7 W by intracavity doubling self-Raman laser of YVO₄/Nd:YVO₄ composite. *Opt. Lett.* **2009**, *34*, 2763–2765. [[CrossRef](#)]
11. Chen, Y.F.; Pan, Y.Y.; Liu, Y.C.; Cheng, H.P.; Tsou, C.H.; Liang, H.C. Efficient high-power continuous-wave lasers at green-lime-yellow wavelengths by using a Nd:YVO₄ self-Raman crystal. *Opt. Express* **2019**, *27*, 2029–2035. [[CrossRef](#)]
12. Lee, A.J.; Spence, D.J.; Piper, J.A.; Pask, H.M. A wavelength-versatile, continuous-wave, self-Raman solid-state laser operating in the visible. *Opt. Express* **2010**, *18*, 20013–20018. [[CrossRef](#)] [[PubMed](#)]
13. Kananovich, A.; Demidovich, A.; Danailov, M.; Grabtchikov, A.; Orlovich, V. All-solid-state quasi-CW yellow laser with intracavity self-Raman conversion and sum frequency generation. *Laser Phys. Lett.* **2010**, *7*, 573–578. [[CrossRef](#)]
14. Chen, Y.F.; Liu, Y.C.; Pan, Y.Y.; Gu, D.Y.; Cheng, H.P.; Tsou, C.H.; Liang, H.C. Efficient high-power dual-wavelength lime-green Nd:YVO₄ lasers. *Opt. Lett.* **2019**, *44*, 1323–1326. [[CrossRef](#)] [[PubMed](#)]
15. Chen, Y.F.; Huang, H.Y.; Lee, C.C.; Hsiao, J.Q.; Tsou, C.H.; Liang, H.C. High-power diode-pumped Nd:GdVO₄/KGW Raman laser at 578 nm. *Opt. Lett.* **2020**, *45*, 5562–5565. [[CrossRef](#)]
16. Chen, Y.F.; Chen, C.M.; Lee, C.C.; Huang, H.Y.; Li, D.; Hsiao, J.Q.; Tsou, C.H.; Liang, H.C. Efficient solid-state Raman yellow laser at 579.5 nm. *Opt. Lett.* **2020**, *45*, 5612–5615. [[CrossRef](#)] [[PubMed](#)]
17. Chen, Y.F. Compact efficient all-solid-state eye-safe laser with self-frequency Raman conversion in a Nd:YVO₄ crystal. *Opt. Lett.* **2004**, *29*, 2172–2174. [[CrossRef](#)]
18. Chen, Y.F. Efficient 1521-nm Nd:GdVO₄ Raman laser. *Opt. Lett.* **2004**, *29*, 2632–2634. [[CrossRef](#)]
19. Fan, Y.X.; Liu, Y.; Duan, Y.H.; Wang, Q.; Fan, L.; Wang, H.T.; Jia, G.H.; Tu, C.Y. High-efficiency eye-safe intracavity Raman laser at 1531 nm with SrWO₄ crystal. *Appl. Phys. B* **2008**, *93*, 327. [[CrossRef](#)]
20. Shen, H.; Wang, Q.; Hu, W.; Chen, X.; Liu, Z.; Cong, Z.; Gao, L.; Tao, X.; Zhang, H.; Fang, J. Compact high repetition-rate actively Q-switched and mode-locked eye-safe Nd:KLu(WO₄)₂/BaWO₄ Raman laser. *Opt. Commun.* **2013**, *311*, 177. [[CrossRef](#)]
21. Huang, J.; Lin, J.; Su, R.; Li, J.; Zheng, H.; Xu, C.; Shi, F.; Lin, Z.; Zhuang, J.; Zeng, W.; et al. Short pulse eye-safe laser with a stimulated Raman scattering self-conversion based on a Nd:KGW crystal. *Opt. Lett.* **2007**, *32*, 1096.
22. Fan, L.; Shen, J.; Wang, X.-Y.; Fan, H.-B.; Zhu, J.; Wang, X.-L.; Wang, H.-T. Efficient continuous-wave eye-safe Nd:YVO₄ self-Raman laser at 1.5 μm. *Opt. Lett.* **2021**, *46*, 3183–3186. [[CrossRef](#)] [[PubMed](#)]
23. Trimble, W.L.; Sulai, I.A.; Ahmad, I.; Bailey, K.; Graner, B.; Greene, J.P.; Holt, R.J.; Korsch, W.; Lu, Z.T.; Mueller, P.; et al. Lifetime of the 7s6d ¹D₂ atomic state of radium. *Phys. Rev. A* **2009**, *80*, 054501. [[CrossRef](#)]
24. Booth, D.W.; Rabga, T.; Ready, R.; Bailey, K.G.; Bishof, M.; Dietrich, M.R.; Greene, J.P.; Mueller, P.; O'Connor, T.P.; Singh, J.T. Spectroscopic study and lifetime measurement of the 6d7p ³F₂^o state of radium. *Spectrochim. Acta Part B Atomic Spectrosc.* **2020**, *172*, 105967. [[CrossRef](#)]
25. Maiman, T.H. Stimulated Optical Radiation in Ruby. *Nature* **1960**, *6*, 4736. [[CrossRef](#)]
26. Sanson, A.; Giarola, M.; Rossi, B.; Mariotto, G.; Cazzanelli, E.; Speghini, A. Vibrational dynamics of single-crystal YVO₄ studied by polarized micro-Raman spectroscopy and ab initio calculations. *Phys. Rev. B* **2012**, *86*, 214305. [[CrossRef](#)]
27. Chen, Y.F.; Lan, Y.P.; Wang, S.C. Efficiently high-power diode-end-pumped TEM₀₀ Nd:YVO₄ laser with a planar cavity. *Opt. Lett.* **2000**, *25*, 1016–1018. [[CrossRef](#)]
28. Chen, Y.F.; Lan, Y.P.; Wang, S.C. High-power diode-end-pumped Nd:YVO₄ laser: Thermally induced fracture versus pump-wavelength sensitivity. *Appl. Phys. B* **2000**, *71*, 827–830. [[CrossRef](#)]
29. Chen, Y.F. Pump-to-mode size ratio dependence of thermal loading in diode-end-pumped solid-state lasers. *J. Opt. Soc. Am. B* **2000**, *17*, 1835–1840. [[CrossRef](#)]